Cell Stem Cell
Article

Targeting Self-Renewal in High-Grade Brain Tumors Leads to Loss of Brain Tumor Stem Cells and Prolonged Survival

Zhe Zhu,[1] Muhammad Amir Khan,[1] Markus Weiler,[2,4] Jonas Blaes,[2] Leonie Jestaedt,[5] Madeleine Geibert,[1] Peng Zou,[1] Jan Gronych,[3] Olga Bernhardt,[1] Andrey Korshunov,[6] Verena Bugner,[3] Peter Lichter,[3] Bernhard Radlwimmer,[3] Sabine Heiland,[5] Martin Bendszus,[5] Wolfgang Wick,[2,4] and Hai-Kun Liu[1,*]

[1]Helmholtz Young Investigator Group, Normal and Neoplastic CNS Stem Cells, DKFZ-ZMBH Alliance, German Cancer Research Center (DKFZ), Im Neuenheimer Feld 280, 69120 Heidelberg, Germany

[2]Clinical Cooperation Unit Neurooncology, German Cancer Research Center (DKFZ), Im Neuenheimer Feld 280, 69120 Heidelberg, Germany

[3]Division of Molecular Genetics, German Cancer Research Center (DKFZ), Im Neuenheimer Feld 280, 69120 Heidelberg, Germany

[4]Department of Neurooncology, University Clinic Heidelberg and German Cancer Consortium (DKTK), Im Neuenheimer Feld 400, 69120 Heidelberg, Germany

[5]Department of Neuroradiology, Heidelberg University Hospital, Im Neuenheimer Feld 400, 69120 Heidelberg, Germany

[6]Department of Neuropathology, Heidelberg University Hospital, Im Neuenheimer Feld 220, 69120 Heidelberg, Germany

*Correspondence: l.haikun@dkfz-heidelberg.de

http://dx.doi.org/10.1016/j.stem.2014.04.007

SUMMARY

Cancer stem cells (CSCs) have been suggested as potential therapeutic targets for treating malignant tumors, but the in vivo supporting evidence is still missing. Using a GFP reporter driven by the promoter of the nuclear receptor tailless (Tlx), we demonstrate that Tlx^+ cells in primary brain tumors are mostly quiescent. Lineage tracing demonstrates that single Tlx^+ cells can self-renew and generate Tlx^- tumor cells in primary tumors, suggesting that they are brain tumor stem cells (BTSCs). After introducing a BTSC-specific knock-out of the Tlx gene in primary mouse tumors, we observed a loss of self-renewal of BTSCs and prolongation of animal survival, accompanied by induction of essential signaling pathways mediating cell-cycle arrest, cell death, and neural differentiation. Our study demonstrates the feasibility of targeting glioblastomas and indicates the suitability of BTSCs as therapeutic targets, thereby supporting the CSC hypothesis.

INTRODUCTION

The cancer stem cell (CSC) hypothesis provides an alternative model to explain the tumor cell heterogeneity (Reya et al., 2001). Like normal somatic adult stem cells, which are distributed in different tissues, CSCs are thought to be the less differentiated populations in malignant tissues and are considered to be the cells that are responsible for the maintenance of tumor tissues, as well as for the relapse of tumors after conventional treatment. In most tumor entities, the existence of CSCs has not been demonstrated in vivo with the genetic cell fate mapping approach, which is the most stringent criterion for the identification of normal tissue stem cells (Clevers, 2011). Using lineage tracing, a very recent study performed in a mouse colon adenoma model showed that Lgr5-expressing cells are CSCs (Schepers et al., 2012). This study provided the first solid evidence for the presence of CSCs in unperturbed primary tumors. The CSC hypothesis rises the anticipation that targeting of CSCs in tumors will lead to an improved clinical outcome because they are thought to be the "root" of growing tumors. However, the in vivo experimental evidence supporting that is still missing in most tumor entities.

Brain tumor stem cells (BTSC) are one of the first CSCs identified in solid tumors (Singh et al., 2003, 2004). CD133 has been suggested to be a useful marker for isolation of BTSCs but the results obtained based on this method are controversial (Clevers, 2011). BTSCs share many similarities with normal neural stem cells (NSCs), i.e., expression of markers like Nestin and CD133, or sphere-forming ability when placed into medium containing growth factors (Vescovi et al., 2006). It would not be surprising if BTSCs could hijack the self-renewal pathway of normal NSCs, and similar results have been found in many other type of tumors (He et al., 2009). Several studies tried to target factors that are known to be important of NSC maintenance during brain tumorigenesis. Inhibitor of DNA binding 1 (Id1) is selectively expressed in NSCs in adult neurogenic niches, namely the subventricular zone (SVZ) and the subgranular zone (SGZ) and Id proteins are shown to be involved in regulation of stem cell self-renewal (Nam and Benezra, 2009). However, deletion of Id1 in mouse brain tumors has modest effects on animal survival, although BTSCs of Id1 mutants have reduced self-renewal capacity in vitro (Barrett et al., 2012). This leads to the assumption that the self-renewal of BTSCs does not predict brain tumor growth potential, however, it is noteworthy that Id1 mutant animals have normal NSCs populations and normal neurogenesis (Barrett et al., 2012). A recent study using a cell ablation approach demonstrated that chemo-resistant Nestin expressing brain tumor cells are responsible for brain tumor propagation, and ablation of these cells led to prolonged survival of tumor-bearing mice (Chen et al., 2012), which support that self-renewing tumor

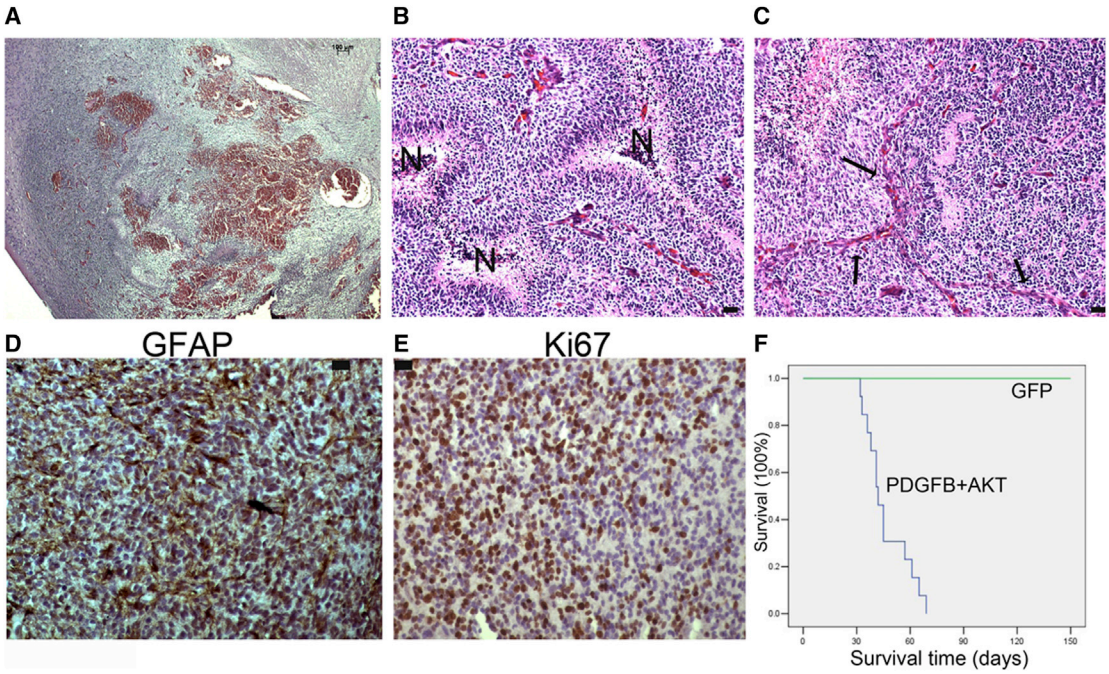

Figure 1. Induction of High-Grade Brain Tumors in Ntv-a Mice

(A) Hematoxylin and eosin (H&E) staining of GB induced with PDGFB and AKT in the Nestin-Tv-a model. Scale bar represents 100 μm.

(B and C) Brain tumors induced with PDGFB and AKT have typical pathological features like pseudopalisading and necrosis (B, N indicates the necrotic areas) and vascular proliferation (C, arrows). Scale bar represents 50 μm.

(D and E) The mouse tumors highly express the astrocyte marker GFAP (D) and the proliferation marker Ki67 (E). Scale bar represents 20 μm.

(F) Kaplan-Meier survival curve of the Ntv-a mice induced with PDGFB and AKT (n = 15). RCAS-GFP was used as control vector (n = 12).

See also Figure S1.

cells are important therapeutic targets of brain tumors in vivo. The nuclear receptor tailless (Tlx, Nr2e1) is specifically expressed in adult NSCs and loss of Tlx in mice leads to the loss of self-renewal of NSCs, both in the SVZ and the SGZ (Liu et al., 2008, 2010; Shi et al., 2004; Zhang et al., 2008; Zou et al., 2012). Interestingly, Tlx is also overexpressed in human brain tumors and it is important for tumor initiation from the SVZ (Liu et al., 2010; Zou et al., 2012). These results suggest that Tlx is a crucial regulator for self-renewal of adult NSCs and brain tumorigenesis. However, the expression pattern and function of Tlx in established tumors is unknown.

To investigate whether BTSCs are important for tumor maintenance and survival, we generated a mouse brain tumor model, which allows cell-type-specific genetic manipulation in fully developed primary brain tumors. We found that the Tlx^+ cells are the slow-dividing and undifferentiated tumor cells in vivo, xenotransplantation, and lineage tracing directly demonstrates that they are the BTSCs. An inducible inactivation of Tlx in Nestin expressing brain tumor cells leads to a significant prolongation of survival of tumor-bearing animals. Tumor cells from Tlx-deficient tumors lost self-renewing capacity and resulted in less proliferating cells. In addition, we identified several important signaling pathways involved in cell-cycle arrest, cell death, and neural differentiation. Overall, this study demonstrates the direct genetic evidence of the importance of CSC in brain tumors and provides an attractive therapeutic target of high-grade gliomas.

RESULTS

A Mouse Model for Gene Targeting in Fully Developed High-Grade Brain Tumors

To establish a mouse model that allows gene targeting in established brain tumors, we made use of the RCAS/tv-a system to initiate brain tumors. The RCAS/tv-a system uses an avian retroviral vector, called RCAS, derived from avian leukosis virus (ALV, subgroup A), and a Nestin-tv-a (Ntv-a) transgenic mouse line that expresses Tv-a (the receptor for ALV-A) under the control of the *Nestin* gene promoter. This system makes it possible to transfer and express exogenous genes in Nestin-expressing neural progenitor cells and their progeny (Holland, 2001). With coinjection of RCAS viruses expressing AKT and platelet-derived growth factor B (PDGFB), we were able to induce high-grade brain tumors with full penetrance in Ntv-a mice (Figure 1A). Approximately 60% of the tumors were multifocal glioblastoma (GB) (Table S1 available online), which have classic histopathologic features of human GB, like pseudopalisading-associated necrosis and vascular proliferation (Figures 1B and 1C). These tumors express the astrocyte marker glial filament acid protein (GFAP) and the cell proliferation marker Ki67 (Figures 1D and 1E). All animals developed brain tumors within 3 months after injection of PDGFB and AKT (Figure 1F). To determine the cell of origin of brain tumors in this model, we injected the RCAS-GFP producing DF-1 cells into the Ntv-a mice, which allow visualization of infected cells with GFP signal. Three days after

injection, we found that most of GFP cells are located in the SVZ area and all express GFAP and Nestin (Figures S1A and S1B), suggesting the radial glia-like NSCs are the cells initially infected. It is known that the SVZ NSCs mainly give rise to newborn neurons in the olfactory bulb. One month after injection, we found many GFP$^+$ cells in the olfactory bulb (Figure S1C), which further demonstrate that the NSCs are targeted by RCAS approach. This is consistent with the working principle of this model that only the Nestin-tv-a-expressing cells are infected by the RCAS vectors (Holland et al., 1998). We also analyzed the tumor location in many animals (Table S1). Most of the tumors are multifocal, but there is no strong correlation between tumor grade and location. Nevertheless, SVZ is the most frequently associated region of tumor locations (Table S1), again suggesting the stem cell origin of these tumors. This mouse model allows induction of tumors without involving Cre/LoxP technology, thus the Cre/LoxP system can be used for additional genetic manipulations in mouse primary brain tumors. We then generated mouse models with the following genotypes, Ntv-a;Tlx-GFP and Ntv-a; Nestin-CreERT2;Tlx$^{flox/flox}$. As we have shown in Tlx-GFP transgenic mice, in which the GFP expression is driven by a Tlx bacterial artificial chromosome (BAC)-based promoter, that NSCs are GFP$^+$ (Feng et al., 2013), we are able to visualize the Tlx expressing brain tumor cells via the GFP signal. Furthermore, the Ntv-a;Nestin-CreERT2;Tlx $^{flox/flox}$ mice can be used to induce Tlx inactivation in PDGFB/AKT-induced brain tumors, in a tamoxifen (TMX)-dependent manner.

Tlx$^+$ Cells in Mouse Brain Tumors Are Slow-Dividing Cells

After induction of tumors in Tlx-GFP;Ntv-a mice, we observed heterogeneous expression of GFP in mouse brain tumors (Figure 2A). To further characterize the Tlx-GFP tumor cells in vivo, we performed additional immunohistochemistry (IHC) analysis, and we found that the GFP$^+$ cells were negative for Olig2 (Figure 2B), a common glioma marker and an oligodendrocyte marker in normal brain tissues. We found that some of the GFP$^+$ cells were also positive for GFAP, which is a marker for mature astrocyte and radial glia like NSCs in adult brain (Figure 2C). GFP$^+$ cells were also negative for doublecortin (DCX), a marker for immature neurons (Figure 2D). We found that a commonly used marker for NSCs, NESTIN, is widely expressed in the mouse tumors and that the Tlx-GFP$^+$ cells are just a subpopulation of NESTIN$^+$ cells (Figure 2E). It has been suggested that CSCs are slow-dividing cells that is one of the major features of many tissue-specific stem cells (Li and Clevers, 2010). By costaining of GFP with the cell proliferation marker Ki67 and another widely used stem cell marker, Sox2, we found that most of the GFP cells were negative for Ki67 (Figure 2F). Interestingly, the majority of the Sox2 cells were negative for Tlx-GFP but positive for Ki67 (Figure 2F). We further quantified the relative distribution of Tlx-GFP cells comparing with three markers (Sox2, GFAP, NESTIN), the result indicates that Tlx-GFP marks a unique population in primary brain tumors (Figure 2G). Using additional cell proliferation markers like proliferating cell nuclear antigen (PCNA) (Figure S2A) or MCM2 (Figure S2B) further confirmed that Tlx$^+$ cells are largely quiescent (Figure 2H). This result suggests that the Tlx-GFP$^+$ tumor cells are not fast-dividing cells in vivo, and it is known that most of the Tlx-expressing cells in the SVZ are slowly dividing in vivo (Liu et al., 2008). This could be further confirmed by bromodeoxyuridine (BrdU) pulse labeling (2 hr) experiments, which showed that a small population (6.3%) of the BrdU-incorporating cells were positive for GFP and around 9.4% of the GFP$^+$ cells incorporated BrdU (Figure 2I). This is consistent with the results obtained by containing of Tlx-GFP with proliferation markers (Figure 2H). BrdU label retention experiments have been used to demonstrate the slow-dividing features of normal stem cells (Bickenbach, 1981). We performed BrdU injections for 3 consecutive days and mice were analyzed 2 weeks after the last BrdU injection, which allowed us to visualize the BrdU label-retaining cells (LRC) in tumor tissues. We observed that most of the BrdU label retaining cells (74.5%) are GFP$^+$ (Figure 2J, arrows), which strongly suggests that Tlx-GFP$^+$ cells are the slow-dividing cells in brain tumors. We also found that the Tlx-GFP$^+$ BrdU LRC cells are positive for GFAP or NESTIN, but are negative for Sox2 (Figures S2C–S2E). The Tlx-GFP$^-$ LRC cells are Olig2$^+$ and Sox2$^-$ (Figures S2F and S2G), suggesting these are the fully differentiated tumor cells.

The neurosphere assay has been widely used for the determination of the existence of self-renewing cells in brain tissues (Singec et al., 2006). Here, we found that when tumor cells are placed into tumorsphere culture medium containing FGF2 and EGF, the vast majority of tumorspheres are GFP$^+$ (Figure 2K). We isolated the Tlx-GFP$^+$ and GFP$^-$ cells via fluorescence-activated cell sorting (FACS) from primary tumors, these two populations were cultured in parallel using tumorsphere culture conditions. We found that only the Tlx-GFP$^+$ cells form tumorspheres and they can be passaged multiple times. The Tlx-GFP$^-$ cells cannot form tumorspheres efficiently and no spheres can be further passaged (Figure 2L).

It is intriguing that many GFP$^+$ cells are located in close proximity to the vasculature as shown by staining of an endothelial marker CD34 (Figure 2M), suggesting that the GFP$^+$ cells are located in a vascular niche. This is further supported by measuring the average distance between GFP cells and CD34$^+$ endothelial cells. The distance is significantly shorter than the distance between Ki67$^+$ and CD34$^+$ cells (Figures 2M and 2N). Although this is in line with a well-recognized feature of BTSCs, the slow-dividing feature of the perivascular cells does not support the notion that the vascular niche is supporting the proliferative capacity of stem cells. These results suggest that Tlx-GFP cells are the bona fide slow-dividing BTSCs in primary brain tumors.

Xenotransplantation and Lineage Tracing Demonstrate that Tlx-GFP Cells Are BTSCs

BTSCs were initially defined as cells that can initiate new tumors when transplanted into immunocompromised mice (Singh et al., 2004). To test whether there is a difference between Tlx-GFP$^+$ and Tlx-GFP$^-$ cells regarding their potential to initiate tumors after transplantation, we performed the following serial transplantation experiment. Tlx-GFP$^+$ and Tlx-GFP$^-$ cells were isolated via FACS. A different number of cells (10^5, 10^4) were injected intracranially into the brains of nude mice. Animals were monitored with a 9.4 Tesla MRI device to determine tumor frequency (Figure 3A). We found that the Tlx-GFP cells form tumors very efficiently upon transplantation, and the tumors

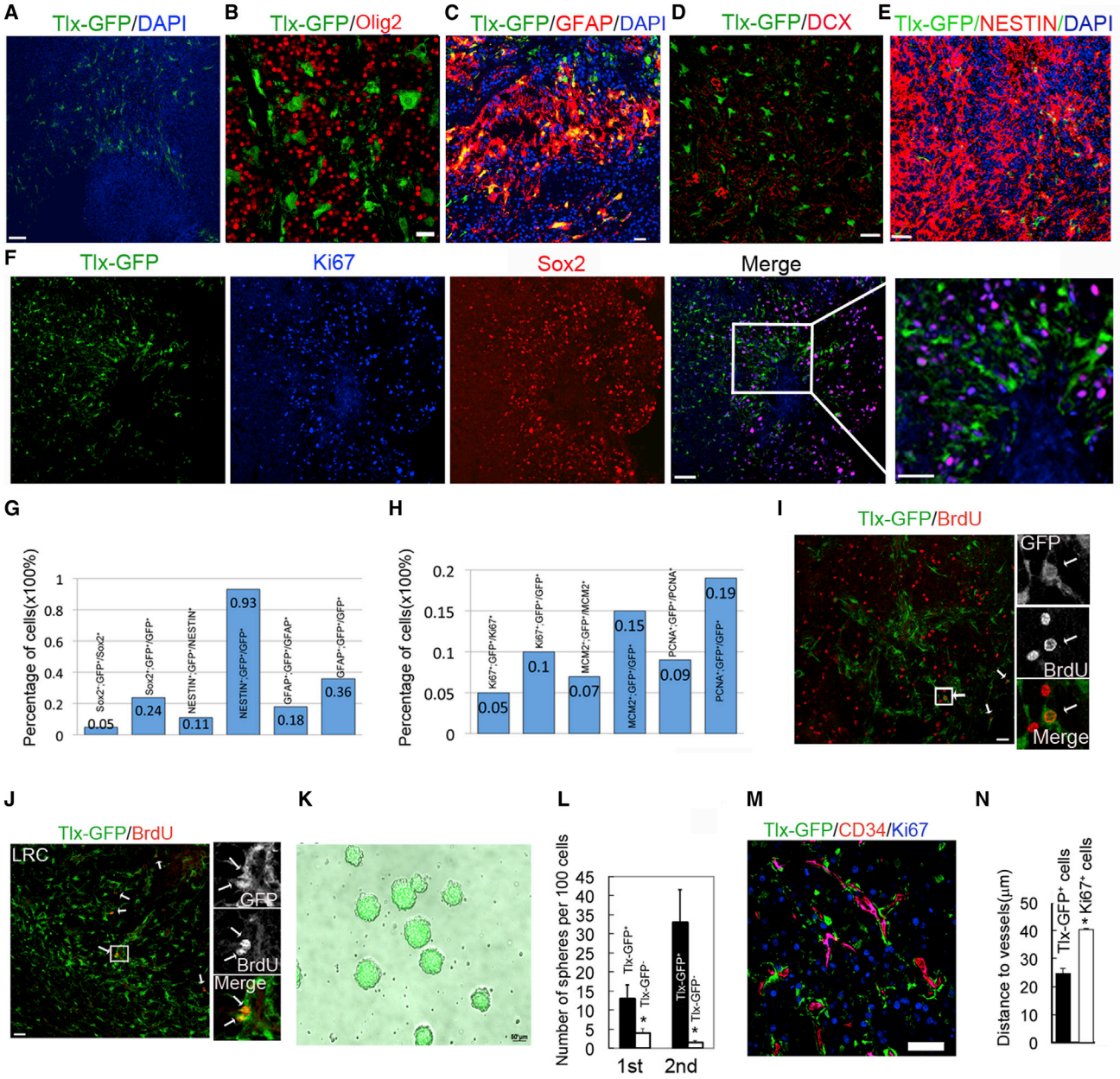

Figure 2. Characterization of Tlx-GFP$^+$ Cells in Primary Mouse Brain Tumors

(A) GFP staining of mouse tumors developed in Ntv-a;Tlx-GFP mouse brain. Note that there is only a subset of tumor cells that are positive for GFP. Scale bar represents 20 μm.

(B–E) Brain tumor sections derived from Ntv-a;Tlx-GFP mouse brain were stained for: GFP (green), Olig2 (red) (B); GFP (green), GFAP (red) (C); GFP (green) DCX (red)(D), and GFP (green), NESTIN (red)(E). Note that there is no colocalization between GFP, Olig2, and DCX. Only a subset of GFAP or NESTIN cells express Tlx-GFP. Scale bars represent 20 μm.

(F) Staining of Ntv-a;Tlx-GFP brain tumor sections with GFP(green)/Ki67(blue)/Sox2(red) antibodies demonstrates that most of the Tlx-GFP cells are negative for Ki67 and Sox2 staining. This suggests they are quiescent in vivo. Note that most of the Ki67$^+$ cells express Sox2. Scale bars represent 50 μm.

(G and H) Quantification of relative distribution of Tlx-GFP$^+$ cells comparing with different markers (G: Sox2, NESTIN, GFAP; H: Ki67, MCM2, and PCNA). Note that none of these markers can exclusively label Tlx-GFP cells.

(I) BrdU labeling was performed to see the proliferation in tumor mice. BrdU injection to Ntv-a;Tlx-GFP tumor-bearing mice was performed 2 hr before sacrificing the mice. BrdU (red) and GFP (green) costaining of tumor sections were performed. Note that only a very small populations of GFP cells are BrdU$^+$ (inset showing a higher magnification of a BrdU and GFP double-positive cell). Scale bar represents 20 μm.

(J) Ntv-a;Tlx-GFP tumor mice received 3 days consecutive BrdU injections and the mice were sacrificed 3 weeks after the last injection. BrdU (red) and GFP (green) costaining of tumor sections were performed. Note that the BrdU label-retaining cells are GFP$^+$ (arrows). Inset: a higher magnification of a BrdU and GFP double-positive cell. Scale bar represents 20 μm.

(legend continued on next page)

recapitulate the histological features of primary tumors, namely pseudopalisading-associated necrosis and vascular proliferation (Figures 3A and 3D). The Tlx-GFP$^-$ cells rarely form tumors upon transplantation of 10^5 cells (Figure 3A). We also analyzed the tumors initiated by Tlx-GFP$^+$ cells. Although we only injected Tlx-GFP-pure population, the heterogeneous expression pattern of Tlx-GFP is reestablished in transplanted tumors and they are still restricted in the slow-dividing subpopulation in primary tumors shown by costaining with PCNA or NESTIN (Figures 3B and 3C). This suggests the GFP$^+$ cells are able to generate GFP$^+$ and GFP$^-$ cells after transplantation. All animals developed tumors after injection of 10^4 Tlx-GFP$^+$ cells, but no tumors were observed with injection of the same amount of Tlx-GFP$^-$ cells (Figure 3D). Most importantly, the tumors initiated by Tlx-GFP$^+$ cells could be serially transplanted up to at least three times during our analysis time (Figures 3E and 3F). The one tumor initiated by the GFP$^-$ population (1/7) can be further transplanted, but the histology analysis indicates that it is a rather benign tumor without the histological features of GB (Figure 3G and 3H). Most importantly, we did not observe Tlx-GFP expression in transplanted tumors from Tlx-GFP$^-$ cells, indicating that reacquiring Tlx-GFP expression is not a frequent event in vivo. This result demonstrated that Tlx-GFP tumor cells can reestablish a heterogeneous tumor upon transplantation. We also performed a similar transplantation experiment using FACS-isolated primary Tlx-GFP$^+$ and Tlx-GFP$^-$ cells. The results are consistent with the experiment described above (Figure S3) suggesting that Tlx-GFP$^+$ cells are the cells that can serially transplant tumors.

The limitation of the xenotransplantation assay has been raised recently (Magee et al., 2012). This prompts us to perform the lineage tracing experiment to visualize the potential of Tlx$^+$ tumor cells. As shown in Figure 3I, Tlx-GFP;Tlx-CreERT2;Ntva; Confetti tumor-bearing mice were treated with TMX to induce Cre-dependent recombination only in the Tlx-GFP cells because Cre is controlled by the Tlx promoter. The confetti mice allow random labeling of cells with one of four random colors upon Cre activation (Snippert et al., 2010). In our model, the tracing was initiated in established tumors, thus no retracing experiment is needed, which is different from the lineage tracing experiment in a colon adenoma model (Schepers et al., 2012). We also showed above that Tlx-GFP cells in the tumor are the tumor cells because they initiate tumors upon transplantation. No recombination was observed without TMX treatment. After low-dosage TMX treatment, we can specifically induce spark-labeling only in the single Tlx-GFP$^+$ cells in side tumor (Figure 3J). In this experiment, the confocal setting can detect all colors during the image acquisition, also excluding clones with mixed colors. Seven days after TMX injection (as shown in Figure 3K, represented by YFP$^+$ clone), we found that most of the clones are two to three cells and they are grouped together. Thirteen days after TMX injection, more cells were found but the cells started to migrate away from each other. It is important to note the glioblastoma is one of the most invasive solid tumors, and our data also demonstrated that invasive feature of these cells. Two months after TMX treatment, we started to see big clones that had infiltrated into different places inside tumors (Figure 3K). This experiment clearly demonstrates that a single Tlx$^+$ tumor cell can generate big clones of tumor cells over the long term. These results, together with the transplantation assay, strongly suggest that Tlx-GFP cells are BTSCs in vivo.

Recently, it was demonstrated that BTSCs are resistant to temozolomide (TMZ) treatment (Chen et al., 2012), most likely because of their slow-dividing feature as we described. To test whether Tlx-GFP cells become activated after TMZ treatment, we applied TMZ as described in Figure 3L and followed with CidU long-term tracing to label the slow-dividing Tlx-GFP cells. IdU was injected into tumor mice 2 hr before analysis. We found that without TMZ treatment, Tlx-GFP/CidU cells did not incorporate IdU during the analysis period, but the TMZ-treated Tlx-GFP/CidU cells became IdU$^+$ indicating that they reentered the cell-cycle after TMZ treatment (Figure 3K). This suggests that these cells are the cell-of-origin of relapsed tumors after chemotherapy.

Inducible Inactivation of Tlx in Brain Tumors Leads to Prolonged Survival

The fact that Tlx is an essential transcription factor for self-renewal of NSCs and for brain tumor initiation from NSCs, led us to investigate whether inactivation of Tlx can serve as a therapeutic strategy for treating GB. We generated the Ntv-a; Nestin-CreERT2;Tlx$^{flox/flox}$ mice for such an experiment. The Tlx-GFP population is also positive for NESTIN (Figure 2I), which suggests that we are able to induce the knockout of Tlx in brain tumors using Nestin-CreERT2 mice, in which a TMX-inducible Cre recombinase is expressed under the *Nestin* promoter. Based on the observation of the survival of PDGFB/AKT-injected animals, we decided to induce Tlx mutation with TMX 10 days before the tumor-bearing animals were expected to develop tumor-related symptoms (i.e., 2.5 weeks after RCAS-PDGFB/AKT injection). We confirmed that high-grade tumors were already developed in those animals at the stage they underwent TMX treatment (Figure 4A; N indicates necrosis, n = 5). Control animals were Ntv-a;Tlx$^{flox/flox}$ mice, which received identical treatment. We observed that the Tlx mutant tumor mice survived significantly longer than the control mice (Figure 4B), suggesting that targeting Tlx in brain tumors is beneficial for the survival of tumor-bearing animals. To confirm whether Cre recombination is efficient in mutant tumors, both RNA and protein were isolated for Tlx expression analysis, and we could confirm that Tlx RNA and protein levels were both significantly downregulated in the

(K) All tumorspheres derived from the Ntv-a;Tlx-GFP tumors are positive for Tlx-GFP, suggesting that only the Tlx-GFP cells can form tumorspheres in vitro. Note that around 94.7% of cells are GFP$^+$ in this culture.
(L) Ntv-a;Tlx-GFP brain tumors were separated into GFP$^+$ and GFP$^-$ populations via FACS before being subjected to tumorsphere culture experiment. Number of spheres formed by 100 cells were quantified. Note that spheres derived from GFP$^-$ can not be further passaged. $p < 0.05$.
(M) Ntv-a;Tlx-GFP brain tumors costained with CD34 (red), Ki67(blue), and GFP (green). Note that most GFP cells are negative for Ki67 and are associated with CD34$^+$ endothelial cells. Scale bar represents 50 μm.
(N) The average distance between Tlx-GFP cells and CD34$^+$ cells is shorter than that between Ki67 cells and CD34$^+$ cells. $p < 0.05$.
See also Figure S2.

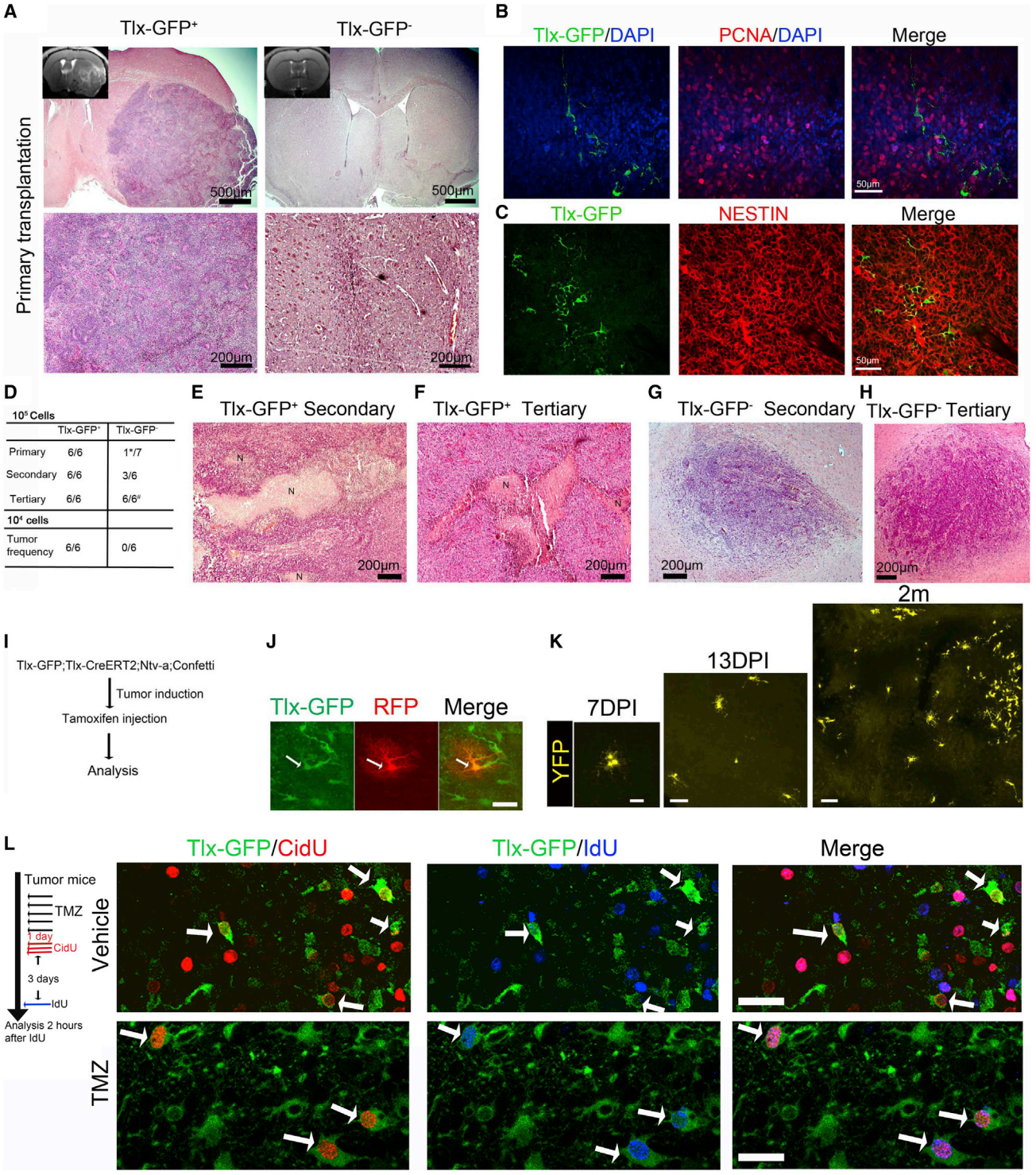

Figure 3. Xenotransplantation and Lineage Tracing Demonstrate that Tlx-GFP Cells Are BTSCs

(A) Tlx-GFP$^+$ or Tlx-GFP$^-$ (10^5) cells were injected into the brain of nude mice. H&E staining indicated that Tlx-GFP$^+$ initiated tumors with GB features, but most of the mice injected with Tlx-GFP$^-$ cells did not develop tumors. Inset: MRI image of transplant-initiated tumors.

(B and C) Tumors initiated by Tlx-GFP$^+$ are heterogeneous. Costaining of Tlx-GFP with PCNA demonstrates that Tlx-GFP$^+$ cells remain to be slow-dividing (B) and it is restricted to a subpopulation of NESTIN expressing cells as in primary tumors (C).

(D) Summary of the transplantation experiment. When injected with 10^5 cells, all Tlx-GFP$^+$-injected animals develop tumors, and these tumors can be serially transplanted at least for three rounds. The one tumor initiated by the Tlx-GFP$^-$ cells can be further transplanted. *Only the animal developed tumor was used for

(legend continued on next page)

mutant tumors at the end point of the survival assay (Figures 4C and 4D). We found that the Tlx mutant tumors were smaller (Figure 4E). It is worth noting that most Tlx mutant animals still showed neurological symptoms and brain tumors could still be observed, although the Tlx mutant brain tumors were much smaller and less infiltrative (Figure 4F). Furthermore, we performed histological analyses of all tumors, and strikingly the majority of the Tlx mutant tumors did not have features of GB (e.g., pseudopalisading and vascular proliferation) (Figure 4G). This could be further confirmed through neuropathological assessment and grading according to the World Health Organization (WHO) classification of CNS neoplasias of all tumors by a trained neuropathologist. Tlx mutant tumors had a lower grade compared to the normal control tumors (Figure 4H). This result also provides a possible link between BTSCs and GB histopathology.

There are still tumor cells in the Tlx mutant mice. To assess the potential of Tlx mutant tumor cells, we performed the transplantation experiment after Tlx ablation. Primary tumors were disassociated and 10^5 primary tumor cells were injected in all the experiments. MRI was used to monitor tumors. The Tlx wild-type (WT) tumor cells transplant tumors very efficiently as shown in Figures 4I–4L. Histology analysis demonstrates that Tlx mutant tumors are very small and benign (Figure 4M), and we did not observe any histological features of GB. Importantly, the WT tumors can be serially transplanted but the Tlx mutant tumor failed to initiate any tumors for the secondary transplantation (Figures 4J, 4K, 4N, and 4O). These results strongly suggest that Tlx is required for tumor propagation in the transplantation assay.

These results suggest that death of animals in the Tlx mutant group was driven by cells derived from BTSCs before TMX treatment, which was sufficient to cause damage of normal brain tissues and animal death as a consequence. To test this hypothesis experimentally, we decided to inactivate Tlx by injecting RCAS-Cre together with PDGFB and AKT to achieve an early deletion of *Tlx* gene during tumor development. We found that many animals did not get tumors in the Cre group compared to the group injected with RCAS-GFP together with PDGFB and AKT (Figure S4). This experiment suggests that early treatment of tumor stem cells will greatly improve treatment outcome.

Tlx Inactivation Leads to Loss of Self-Renewing BTSCs

To analyze the cellular consequences in the primary tumor after Tlx deletion, we analyzed the cell proliferation in the tumors after the animals were sacrificed because of brain tumor-related symptoms and found that there were significantly less Ki67-expressing cells in the Tlx mutant tumors. This suggests there was a reduced proliferation upon Tlx deletion (Figure 5A). As Tlx is only expressed by the slow-dividing cells in brain tumors, we hypothesized that the decrease in $Ki67^+$ cells in Tlx mutant tumors was the consequence of Tlx inactivation in BTSCs. Interestingly, when we analyzed tumors 5 days after TMX injection, we found that the number of $Ki67^+$ cells was not changed in the Tlx mutant tumors. This suggests that loss of Tlx results in a decreased generation of $Ki67^+$ proliferating cells (Figure 5B). To further investigate whether loss of Tlx leads to an impaired function of BTSCs, we performed a tumorsphere assay, which showed that Tlx mutant tumors generate significantly less tumorspheres (Figures 5C and 5D), and the mutant tumorspheres could not be further passaged and expanded (Figure 5D). To determine whether this is due to the loss of Tlx in BTSCs, we performed the tumorsphere culture assay using cells derived from the Ntv-a;Nestin-CreERT2;$Tlx^{flox/flox}$ tumors. Seventy-two hours after adding 4-hydroxytamoxifen (4-OHT) to the tumorsphere culture medium to induce Tlx deletion in vitro, we confirmed that Tlx was successfully removed from the cells (Figure 5E). We found that the Tlx mutant tumorspheres could not be passaged as efficiently as Tlx^+ tumor spheres (Figures 5E and 5F), suggesting that loss of Tlx in BTSCs leads to loss of self-renewal. To investigate whether loss of Tlx leads to an altered differentiation capacity of BTSCs, we established adherent cell cultures from untreated Ntv-a;Nestin-CreERT2;$Tlx^{flox/flox}$ tumors. After treatment with 4-OHT, the growth factors were removed from the medium to induce the differentiation process. We found a reduction of glial differentiation in Tlx mutant cells shown by GFAP or Olig2 staining (Figures 5G and 5H), whereas neuronal lineage differentiation was increased in Tlx mutant BTSCs shown by DCX staining (Figure 5I). These results demonstrated that loss of Tlx in primary brain tumors leads to loss of self-renewal and induction of neuronal differentiation, which may explain the survival effect of targeting Tlx in mouse gliomas.

Loss of Tlx in Brain Tumors Leads to the Induction of Pathways Regulating Apoptosis, Senescence, and Differentiation

To investigate the molecular pathways that are altered after Tlx mutation in brain tumors, RNA was isolated from control and mutant tumors and subjected to microarray analysis providing insights into genome-wide expression changes after Tlx inactivation. Interestingly, many pathways involved in cell-cycle regulation, apoptosis, neural differentiation, and senescence were significantly altered (Table S2). Quantitative RT-PCR (qRT-PCR) analysis for some of the candidate genes confirmed that

secondary transplantation, six animals received cells from Tlx-GFP^- tumor and three developed tumors. #All tumors are low grade tumors. When injected with 10^4 cells, only the Tlx-GFP^+ cells initiated tumors.

(E–H) H&E staining of tumors from the serial transplantation experiment. Note that the Tlx-GFP^+ secondary and tertiary tumors have histological features of a GB (E and F), like necrosis (N), which was never observed from the Tlx-GFP^--derived tumors (G and H).

(I–K) Lineage tracing of Tlx^+ cells in primary tumors. (I) Experimental scheme. (J) TMX induction of single cell recombination in Tlx-GFP tumor cells. GFP indicating Tlx^+ cells, RFP indicating cells being labeled by Cre recombination. (K) Representative picture of clone growth over time initiated by a Tlx^+ stem cell labeled with YFP after TMX treatment. Scale bars represent 20 μm if not indicated.

(L) Tlx-GFP tumor-bearing mice received TMZ treatment as described. CidU were injected into these mice 1 day after TMZ treatment, and three injections were performed in 1 day with 2 hr intervals. Three days later, animals were injected with IdU 2 hr before sacrificing. Brain sections were stained using antibodies against CidU(red), IdU(blue)n and GFP (green). Note that in the vehicle-treated brains, GFP/$CidU^+$ cells do not incorporate BrdU indicating they are slow-dividing (arrows), but in the TMZ-treated brains, GFP/$CidU^+$ cells incorporate IdU indicate that they reenter cell-cycle (arrows).

See also Figure S3.

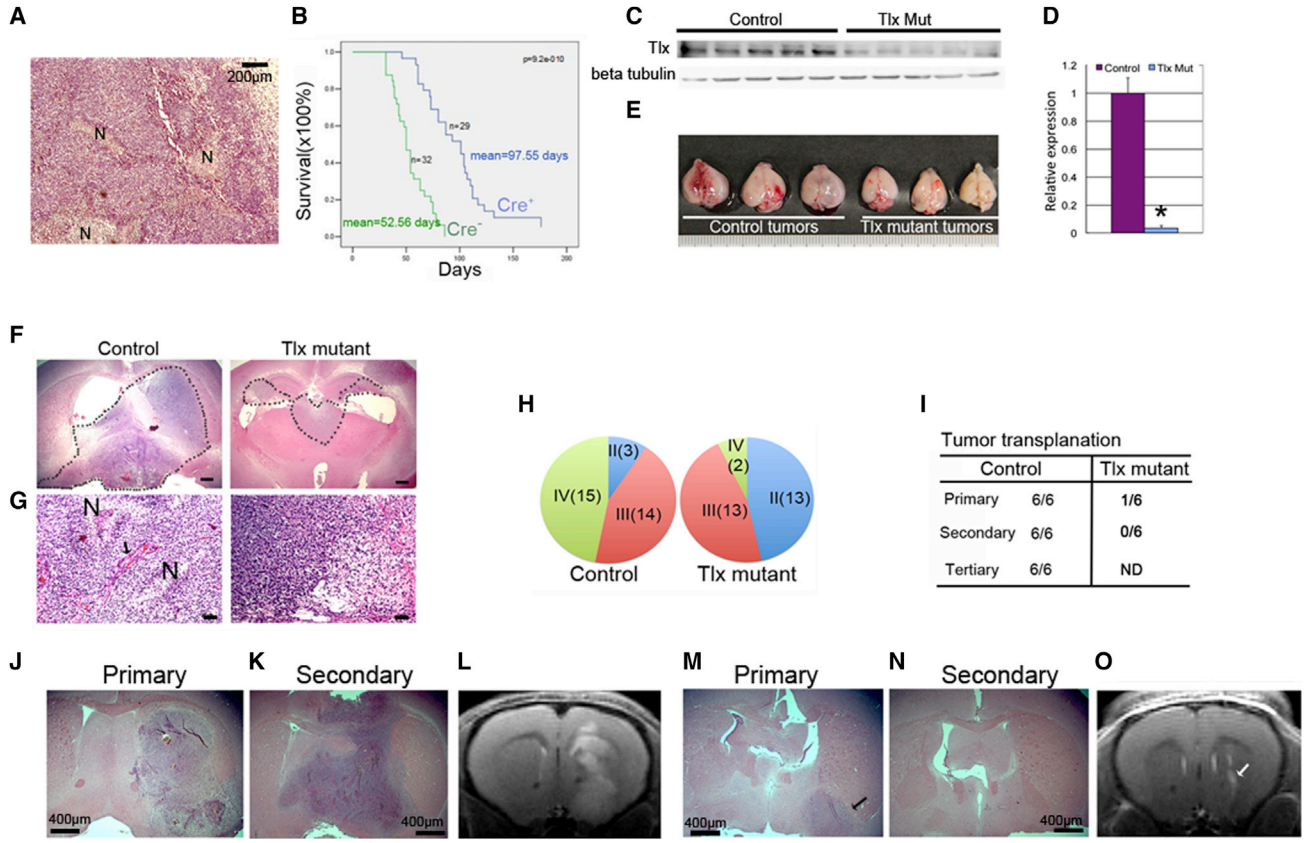

Figure 4. Genetic Inactivation of Tlx in BTSCs Leads to the Loss of Self-Renewing BTSCs and Prolonged Survival

(A) H&E staining demonstrates that malignant brain tumors were already developed at the time point of receiving TMX injection. N, necrosis.

(B) The Kaplan-Meier survival curve of mice receiving TMX. Note that inactivation of Tlx via TMX leads to a significant prolongation of animal survival. (p = 9.2E–10E).

(C and D) RNA and protein were extracted from tumors of animals that were sacrificed at the onset of neurological symptoms. qRT-PCR analysis (C) demonstrating that Tlx is efficiently deleted upon TMX treatment.(n = 6, $p < 0.0001$), This can be confirmed by the western blot results indicating that Tlx protein is absent in the mutant tumors. Data are represented as mean ± SD if not specified.

(E) Brains obtained from Tlx wild-type tumors and Tlx mutant tumors.

(F and G) H&E staining of brain tumors after Tlx inactivation, tumor region was marked with a dash line. Note that the Tlx mutant tumors are much smaller and lack glioblastomas histological features like necrosis (N) associated with pseudopalisading and vascular proliferation (arrow). Scale bars represent 200 μm (F) and 50 μm (G).

(H) WHO classification of Tlx mutant and control brain tumors. Note that there are much less grade IV GBs in the Tlx mutant group.

(I) Tumor cells were isolated before TMX treatment and subjected to stem cell culture condition, 4-OTH was used for induction of Tlx mutation, and 10^5 cells of control and Tlx mutant were collected and injected to the nude mice brains. MRI were used to determine tumor frequency. Note that WT tumors can be serially transplanted, and Tlx mutant tumor cells can not initiate any tumors for the secondary transplantation experiment. *All Tlx mutant cell initiated tumors are local and do not shown any invasive pattern under MRI.

(J–O) Histology of transplanted tumors from the experiment described in (I). Note that high grade tumors can be initiated with WT cells (J and K), which can be clearly visualized with 9.4 tesla MRI, whereas the tumor initiated from the Tlx mutant population is very small (M, arrow) and can not be further transplanted (N). No tumor can be seen with the MRI for the secondary transplantation (O, arrow indicates the injection site).

See also Figure S4.

several important tumor suppressor genes were significantly upregulated. For instance, CDKN2A, CDKN2B, and PML are all upregulated in the Tlx mutant tumors (Figures 6A–6C), suggesting a general inhibition of tumor growth and induction of cell-cycle arrest and cell death after Tlx inactivation. Also, we confirmed that factors that are important for neuronal differentiation were induced in the Tlx mutant tumors as well, for example SMACC1, Dlx2, and TGFβR1 (Figures 6D–6F). These results suggest that loss of Tlx leads to the induction of cell death and differentiation pathways, which is consistent with the phenotype we observed in the mice brain tumors. Dlx2 and TGFβR1 have been suggested as essential regulators for neuronal differentiation (Brill et al., 2008; Shah et al., 1996), which explains in part the increase of neuronal differentiation of Tlx mutant BTSCs (Figures 5G–5I).

The microarray data reflects general changes of genes in a mixed population. To further determine which molecular pathways were altered in BTSCs after Tlx deletion, we isolated the BTSCs from Nestin-CreERT2;$Tlx^{flox/flox}$;Ntva tumor mice untreated with TMX. The cells are cultured under monolayer

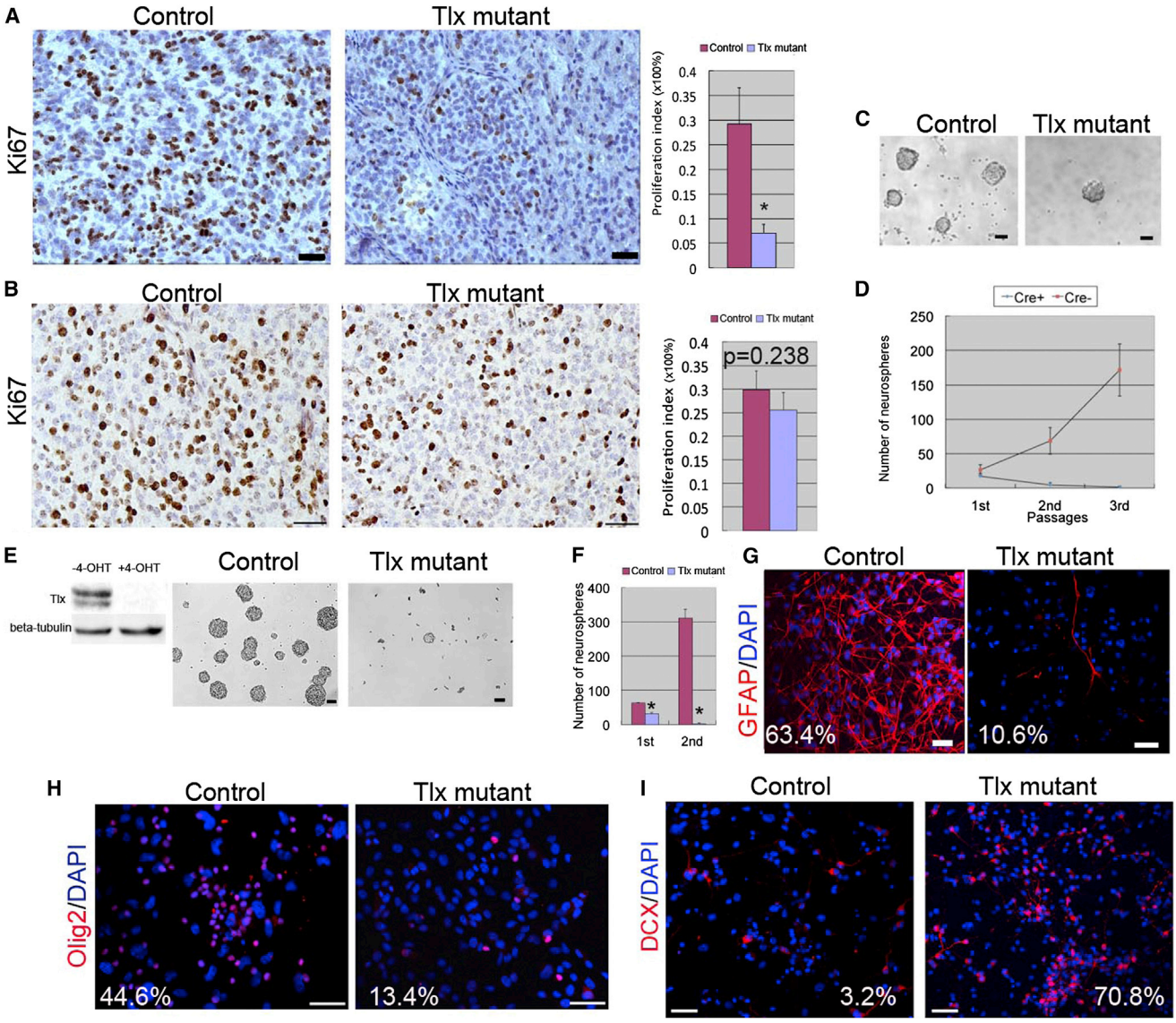

Figure 5. Loss of Tlx in BTSCs Leads to the Loss of Self-Renewal and Induction of Neuronal Differentiation

(A) Ki67 staining of Tlx mutant and control brain tumors. Proliferation index means percentage of Ki67$^+$ cells in tumors (n = 4, $p < 0.01$). Scale bar represents 50 μm.

(B) Five days after TMX induction of Tlx mutation, brain tumors were analyzed for Ki67 staining. Note that no significant differences were observed between normal tumors and Tlx mutant tumors. (n = 4, p = 0.238). Scale bar represents 50 μm.

(C and D) Fewer tumorspheres were derived from Tlx mutant tumors (C). Tumorspheres obtained from Tlx mutant tumors cannot be passaged in vitro whereas control tumorspheres can be passaged and expanded (D). Scale bars represent 50 μm.

(E and F) Tumorsphere culture from the Ntv-a;Nestin-CreERT2;Tlx$^{flox/flox}$ tumors untreated with TMX. 4-OTH was added to the tumorspheres culture medium to induce Tlx mutation in vitro. Western blot shows that Tlx can be efficiently removed after 72 hr of 4-OTH treatment (E). Much less tumorspheres were obtained from Tlx mutant cells after the first passage (E), the Tlx mutant tumorspheres cannot be further passaged and expanded (F, $p < 0.001$ both in the first and second passages). Scale bars represent 50 μm.

(G–I) 4-OTH was added to adherent culture of the Ntv-a;Nestin-CreERT2;Tlx$^{flox/flox}$ tumors. Growth factors were then removed to induce differentiation. Antibodies against GFAP (G), Olig2 (H), and DCX (I) were used for staining of differentiated cells. Note that there are less GFAP and Olig2$^+$ cells in the Tlx mutant culture, but an increase of DCX$^+$ cells was observed in the Tlx mutant culture. Scale bars represent 50 μm.

condition and 4-OHT treatment was performed in vitro that allowed inactivation of Tlx in BTSCs (Figure 6G). We also included two known Tlx target genes (PTEN and p21) that were reported to be repressed by Tlx (Sun et al., 2007; Zhang et al., 2006). RNA expression analysis shown in Figure 6G suggests that as known Tlx target genes, only p21 (CDNK1A), but not PTEN, is upregulated upon Tlx inactivation in BTSCs. PML, TGFβR1, SMARCC1, and DCX are upregulated suggesting that these genes are initially upregulated in Tlx mutant BTSCs, although it is not known yet whether the expression of these genes are repressed by Tlx protein directly, whereas CDKN2A and CDKN2B are not altered in Tlx mutant BTSCs (data not

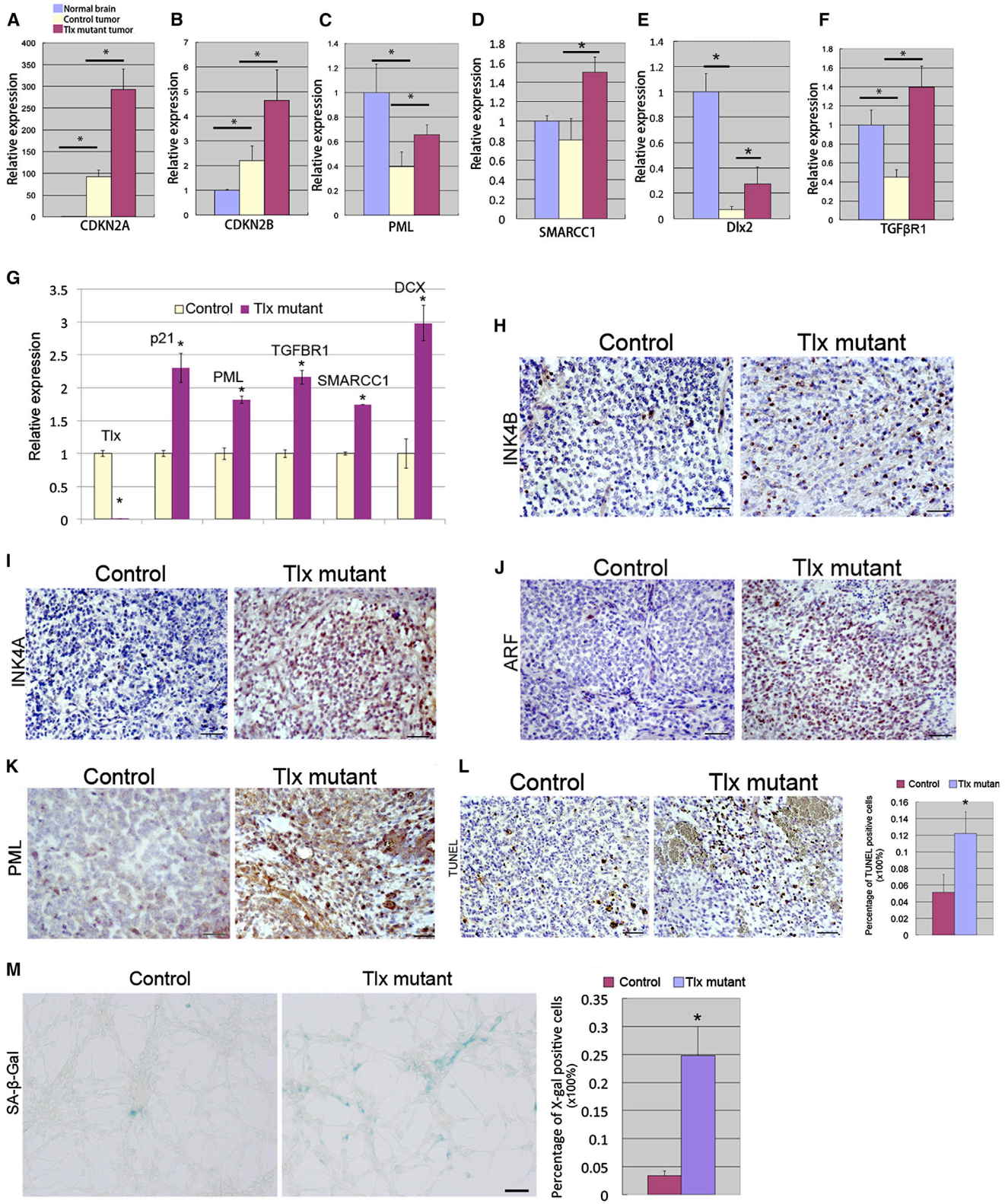

Figure 6. Loss of Tlx in Brain Tumors Leads to Changes in Multiple Essential Pathways Regulating Apoptosis, Senescence, and Differentiation

(A–F) qRT-PCR assay using RNA isolated from normal brain, control, and Tlx mutant tumors. Results show the induction of the expression of CDKN2A, CDKN2B, PML, SMARCC1, Dlx2, and TGFβR1 in Tlx mutant tumors (n = 6 for each group, $p < 0.05$).

(legend continued on next page)

shown), suggesting that the upregulation of these two genes are secondary consequences upon Tlx deletion in primary tumors. It is important to note that we have shown that Tlx overexpression in NSCs does not lead to changes of CDKN2A/CDKN2B expression (Liu et al., 2010), which is consistent with the current results.

It is intriguing that we found factors like p21, CDKN2A, CDKN2B, and PML are all upregulated in the Tlx mutant, although not necessarily only in BTSCs. Additionally, we confirmed the upregulation of CDKN2A (ARF/INK4A), CDKN2B (INK4B), and PML in Tlx mutant tumors by IHC (Figures 6H–6K), suggesting upregulation of these genes in many tumor cells. These factors are known to be involved in the regulation of cell-cycle arrest, apoptosis, and senescence (Gil and Peters, 2006; Sharpless and DePinho, 2007). To investigate whether any of these phenotypes is induced in the Tlx mutant tumors, we first analyzed apoptosis in the Tlx mutant brain tumors. TUNEL assay was performed, and we found that there was a significant increase of TUNEL$^+$ cells in the Tlx mutant tumors (Figure 6L), suggesting that loss of Tlx also leads to an increase in apoptosis of tumor cells. Furthermore, in order to detect whether there is a senescence phenotype after Tlx inactivation, we performed senescence-associated beta-gal (SA-β-Gal) staining on tumor sections. However, we could not detect any cellular senescence in situ (data not shown). One explanation could be that the cells that underwent senescence had been already removed by macrophages from the primary tumors (Kay, 1975). To further investigate whether there was an induction of senescence, we isolated BTSCs from Nestin-CreERT2;Tlx$^{flox/flox}$;Ntv-a tumor animals that have not been treated with TMX. We treated the cells with 4-OHT for 72 hr as described above, 4 days after removal of 4-OHT from the medium, the SA-β-Gal assay was performed. We observed an increase of β-Gal$^+$ cells in the Tlx mutant culture (Figure 6M), indicating an induction of senescence after inactivation of Tlx in BTSCs. The senescence phenotype is likely caused by activation of p21 in BTSCs. These results suggest that the p21, INK4A/ARF, INK4B, and PML pathways are induced upon removal of Tlx in BTSCs, which leads to prolonged survival of tumor-bearing mice.

Tlx Is Important for Self-Renewal of Human BTSCs

We have shown previously that Tlx is upregulated in human brain tumors (Liu et al., 2010). Most importantly, by analyzing the Cancer Genome Atlas (TCGA) data set (http://hgserver1.amc.nl/cgi-bin/r2/main.cgi), we found that Tlx high expression correlates with poor survival in human GB patients, indicating that Tlx is a prognosis marker and a therapeutic target for human GB (Figure 7A).

To investigate whether loss of Tlx in human BTSCs will lead to similar phenotype as we observed in mice, we obtained three different patient-derived human glioblastoma stem cells. Two small hairpin RNAs (shRNAs) against the human *Tlx* gene were used for knock down (KD) of Tlx in human BTSCs, as shown in Figure 7B. Tlx expression is silenced by the two independent shRNA constructs, using shRNA against luciferase as control. We then analyzed the sphere formation ability of Tlx KD human BTSC. Similar to the results in mouse BTSCs, we found that Tlx inhibition leads to loss of sphere-forming ability and a decrease of proliferation of human BTSCs (Figures 7C, 7D, and S5), and no Tlx-KD cells can be passaged three times for further analysis. We then analyzed genes that are changed in Tlx mutant mouse cells. p21 and PML were found to be upregulated in Tlx KD cells, which explains the sphere-forming results. We also found that Tlx KD leads to upregulation of TGFβR1 and Dlx2, suggesting an increase of neuronal differentiation, as we have seen in the mouse mutant cells (Figure 7E). We did not observe changes of CDKN2A, CDKN2B, SMARCC1, and PTEN (data not shown). These results suggest that Tlx is important for the regulation of human BTSCs.

Here, we demonstrate that Tlx is expressed in slow-dividing BTSCs of primary brain tumors by using a mouse somatic brain tumor model. Lineage tracing of single Tlx$^+$ cells in vivo demonstrate they are BTSCs. We also achieved BTSC-specific genetic targeting of Tlx in established brain tumors and showed that Tlx is essential for brain tumor maintenance and survival of tumor-bearing mice (Figures 7H and 7I). These results strongly support the CSCs hypothesis and provide direct evidence of improved animal survival after targeting BTSC.

DISCUSSION

Cancer Stem Cells Are Suitable Therapeutic Targets

The CSCs hypothesis is under intensive debate. One major reason is that markers used for CSCs isolation are not reproducible, which may reflect the genetic and phenotypic heterogeneity of malignant cells or transient expression of these markers. The scientific community faced similar problems when they started to identify adult stem cells in different organs and tissues. The controversies were later alleviated mostly by using animal models, which allow genetic manipulation of particular cell types and follow their behavior for a life-long time (Kretzschmar and Watt, 2012). Recently, several studies were published, which demonstrated the existence of CSC-like cells in different tumor entities using different genetic tools (Chen et al., 2012; Driessens et al., 2012; Schepers et al., 2012). These studies strongly suggest the existence of a differentiation hierarchy in primary tumors. Here, we demonstrated that in a mouse glioma model, a subset of glioma cells expressing the functional NSC marker Tlx, and these cells are slow-dividing in vivo. The Tlx-GFP cells are the cells that can form long-term self-renewing spheres

(G) 4-OHT was added to adherent cultures of the Ntv-a;Nestin-CreERT2;Tlx $^{flox/flox}$ tumors to induce Cre recombination. RNA was collected for qRT-PCR assay, Tlx can be efficiently removed by 4-OHT treatment. Results show that p21, PML, TGFβR1, SMARCC1, and DCX are induced upon Tlx inactivation in BTSCs.
(H–L) Mouse brain tumors were stained for INK4B (H), INK4A (I), ARF (J), and PML (K). All the four proteins were upregulated in the Tlx mutant tumors. Scale bars represent 50 μm in (H–J) and 20 μm in (D).
(L) TUNEL assay demonstrated that there are more apoptotic cells in Tlx mutant brain tumors ($n = 4$, $p < 0.01$). Scale bar represents 50 μm.
(M) 4-OHT was added to adherent cultures of the Ntv-a;Nestin-CreERT2;Tlx $^{flox/flox}$ tumors to induce Cre recombination, a senescence-associated β-gal assay (SA-β-Gal) was performed. Note that there are more SA-β-Gal$^+$ cells in Tlx mutant culture ($n = 4$, $p < 0.01$). Scale bar represents 50 μm.
See also Table S2.

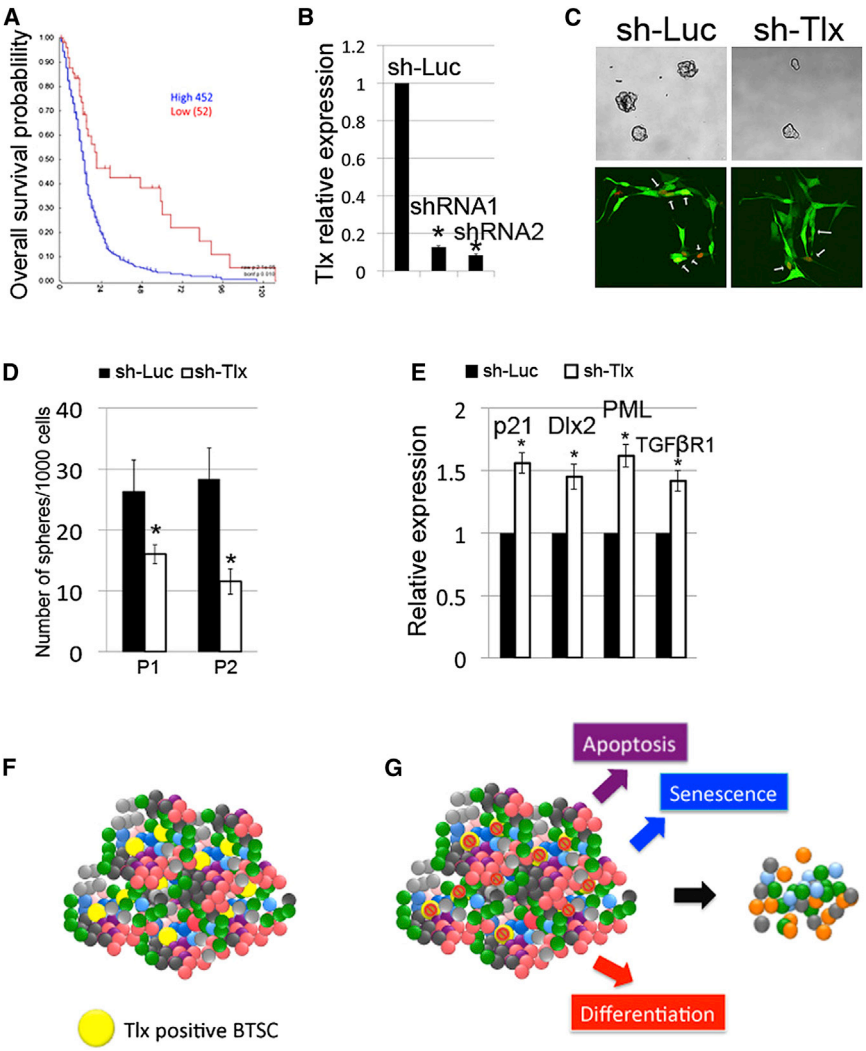

Figure 7. Tlx Is a Therapeutic Target in Human BTSCs

(A) The Kaplan-Meier survival curve of GB patients from the TCGA database. Note that patients with higher Tlx expression have a worse survival rate than patients with lower Tlx expression ($p < 0.05$).

(B) Knock-down (KD) of Tlx expression in human BTSCs was achieved by using two independent shRNAs against human Tlx ($p < 0.05$).

(C and D) KD of Tlx in human BTSCs (T269) leads to loss of sphere forming ability and decrease of cell proliferation measured by BrdU (red) assay. (D) Arrow indicates GFP/BrdU double-positive cells). BrdU was added to the medium for 3 hr before analysis, GFP indicates the shRNA-infected cells ($p < 0.05$ for passage 1 and passage 2).

(E) KD of Tlx leads to upregulation of p21, Dlx2, PML, and TGFβR1 expression in human BTSCs ($p < 0.05$).

(F and G) Graphic illustration of Tlx expression is restricted to the slow-dividing BTSCs (F). Removal of Tlx in the BTSCs leads to regression of brain tumors (G) through induction of differentiation, senescence, and apoptosis pathways.

See also Figure S5.

in vitro. We also performed lineage tracing experiments to show that Tlx$^+$ cells can generate large tumor clones over 2 months. Most importantly, we showed that inactivation of Tlx in brain tumors leads to a prolongation of survival of tumor-bearing animals. This is, in part, due to the induction of several key pathways, which are important for the regulation of senescence, apoptosis, cell-cycle, and differentiation (Figures 7F and 7G). This suggests that the tumor maintenance is dependent on the BTSC population, and loss of this tumor-seeding population will lead to regression of the tumor mass. This directly demonstrates that BTSCs are important for tumor progression and survival.

Nevertheless, it is noteworthy that the Tlx mutant tumors do not disappear. There are several possible explanations of this result. First, the gene targeting of Tlx in BTSCs was initiated in Tlx expressing slow-dividing cells, and the proliferating cells are not affected at the beginning of the targeting (Figure 5B). These cells can still drive the tumor growth until they are exhausted. This growth is causing neurological symptoms in the Tlx mutant mice and this was further supported by the results obtained by inactivating Tlx at early time point (Figure S4). Second, there could be another Tlx-independent BTSC population, which can compensate the effect of Tlx loss, although our serial transplantation experiment showed that Tlx mutant tumor cells cannot be serially transplanted. Third, it could be possible that some Tlx$^+$ cells escaped TMX-induced Cre recombination and later contributed to tumor growth. However, we did not observe reappearance of Tlx for a long time after the last TMX treatment, which does not support this hypothesis. Thus we would favor the first explanation for this phenotype.

Role of Tlx in Normal and Cancer Stem Cells

It was known that Tlx is important for adult NSC maintenance in the SVZ (Liu et al., 2008) and that overexpression of Tlx leads to glioma initiation in mouse models when combined with p53 mutations (Liu et al., 2010). High expression of Tlx was found in different types of tumors in the CNS, including astrocytoma, ependymoma, and GB (Liu et al., 2010). Here, we directly demonstrated that Tlx is also important for BTSCs maintenance. These results suggest that Tlx is an essential regulator and marker for stem cell features in BTSCs. It is interesting to see that inactivation of Tlx in tumors leads to the induction of pathways involved in regulation of cell death, cell-cycle, and neuronal differentiation. We observed that the Tlx target gene *p21*, which is an essential factor mediating cell-cycle arrest and senescence (Rowland and Peeper, 2006), is upregulated both in mouse and human BTSCs upon removal of Tlx, suggesting this is a very conserved pathway. To our knowledge, it has never been shown that Tlx inhibits the INK4A/ARF pathway in normal NSCs, and we

did not see changes of INK4A/ARF expression in Tlx overexpressing NSCs (Liu et al., 2010). This suggests that the upregulation of INK4A/ARF upon inactivation of Tlx is tumor-specific. It was shown that Tlx represses expression of PTEN, which are thought to be essential for maintaining NSC proliferation (Zhang et al., 2006). Here, we did not observe PTEN upregulation in the mutant tumors from the microarray analysis. One possible explanation is that PTEN is silenced or mutated in the AKT+PDGFB-induced high-grade mouse GBs by other mechanisms, which occurs often in human GB patients as well (Furnari et al., 2007).

Taken together, we demonstrated here that Tlx is an essential indicator and regulator of BTSCs. The mouse models we generated provide additional approaches for therapeutic target validation. We also demonstrated that Tlx is a prognosis marker for poor survival of human GB patients, which together with our mouse data suggest that Tlx is a promising therapeutic target for brain tumors. Another advantage of targeting Tlx in brain tumor is that Tlx expression is restricted to the CNS system (Monaghan et al., 1995) and hence an inhibitor that is specifically blocking Tlx activity will have few side effects. As many other nuclear receptors, Tlx is very likely a druggable protein.

EXPERIMENTAL PROCEDURES

Animal Experiments

Mice were housed according to international standard conditions and all animal experiments complied with local and international guidelines for the use of experimental animals. The Ntv-a mouse was kindly provided by Eric Holland. Tlx $^{flox/flox}$ animals was generated as described (Belz et al., 2007). The Nestin-CreERT2 animal was generated as described elsewhere and has been successfully used to target both SVZ and SGZ NSCs via tamoxifen injection (Corsini et al., 2009). Tlx-GFP reporter animal was obtained from the GENSAT project (Gong et al., 2003). Confetti mice were from Jackson Laboratory. Tamoxifen (Sigma) was dissolved in sunflower seed oil (Sigma) with 10% $EtOH_{abs}$ to prepare a 10 mg ml^{-1} solution. Intraperitoneal injections were performed with 1 mg/day for 10 days. BrdU, CidU, or IdU (Sigma) were dissolved in sterile 0.9% saline to prepare a 15 mg ml^{-1} solution, and mice were injected intraperitoneally with 300 mg kg^{-1} 2 hr before sacrifice or with 100 mg kg^{-1}/day for 3 days as described in this article. TMZ (Sigma) was dissolved in DMSO and freshly diluted in 0.9% saline (5 mg/ml) and injected intraperitoneally with 100 mg kg^{-1}/day for 5 days.

RNA Isolation, RT-PCR, and Microarray

RNA from cultured NSCs and dissected mouse tumors and normal brain tissues (mixture of tissues from olfactory bulb, cortex, striatum, hippocampus, and hypothalamus) were isolated with RNeasy Mini Kit (QIAGEN) and transcribed into cDNA using random primers (dN6, Roche). cDNA were quantified with RT-PCR using TaqMan gene expression assays (Applied Biosystems). The levels of four housekeeping genes including ActB, GAPDH, HPRT, and PPIA were averaged and used for normalization. For the microarray experiment, the quality of total RNA was checked by gel analysis using the total RNA Nano chip assay on an Agilent 2100 Bioanalyzer (Agilent Technologies GmbH). Only samples with RNA index values >7 were selected for expression profiling. The analysis is done with R on the GeneView data produced by the scanner.

Cell Culture

Mouse brain tumors were dissected and then digested with Accutase (Sigma-Aldrich). Dissociated cells were grown to neurospheres in DMEM/F12 medium containing 20 ng ml^{-1} EGF (Sigma-Aldrich), 10 ng ml^{-1} FGF2 (Sigma-Aldrich), B27 (GIBCO), and ITSS (Roche). To establish monolayer culture, neurospheres were dissociated with Accutase (Sigma-Aldrich) and were seeded on laminin (Roche) and poly-L-lysine (Sigma-Aldrich)-coated cell culture plates. For the differentiation of NSCs, NSCs were dissociated with Accutase, and 2.5 × 10^4 cells were seeded on laminin and poly-L-lysine-coated coverslips in one well of a 24-well plate. Cells were cultured for 14 days in NSCs medium without EGF and with 5 ng ml^{-1} FGF2. After 14 days, cells were collected for analysis. Medium was renewed every 3 days for the whole procedure. For in vitro CreERT2 induction, 4-hydroxytamoxifen (4-OHT, H7904; Sigma) was dissolved in ethanol at a final stock concentration of 10 mM and kept in single-use aliquots in the dark at –20°C and added freshly to the medium. To induce Cre activity in CreERT2-expressing BTSCs, medium was replaced with the same medium but containing 5 M 4-OHT for 72 hr, then the medium was again replaced with fresh medium without 4-OH for 4 days.

Immunohistochemistry and Western Blot

Mice were perfused with 4% paraformaldehyde, and the brains were postfixed overnight at 4°C. Vibratome sections (50 μm) or 5μm paraffin sections were blocked in 5% normal swine serum in PBST (PBS + 0.2%, Triton X-100) and incubated overnight at 4°C with the primary antibody. The apoptosis assay was performed by using the ApopTag Plus Peroxidase In Situ Apoptosis Kit (Chemicon). The senescence analysis was carried out by using the Senescence β-Galactosidase Staining Kit (Cell Signaling). Fluorescent images were captured using a confocal laser-scanning microscope (LSM700, Zeiss). Statistically significant results were followed up with Student's t tests. For western blot, protein extracts cultured brain tumor stem cells were subjected to electrophoresis and transferred onto a PVDF membrane for immunoblot analysis. The following antibodies were used: Tlx (1:500, rabbit), beta tubulin (1:1,000; Cell Signaling).

ACCESSION NUMBERS

The microarray data have been deposited in the NCBI Gene Expression Omnibus (http://www.ncbi.nlm.nih.gov/geo) and are accessible through GEO Series accession number GSE46125.

SUPPLEMENTAL INFORMATION

Supplemental Information includes Supplemental Experimental Procedures, five figures, and two tables and can be found with this article online at http://dx.doi.org/10.1016/j.stem.2014.04.007.

ACKNOWLEDGMENTS

We thank Günther Schütz for providing mice, the Imaging Facility of the Deutsches Krebsforschungszentrum (DKFZ) and the Carl Zeiss Imaging Center at the DKFZ for their support with image acquisition, the DKFZ Genomic Facility for their support in the microarray experiment, Eric Holland for providing the RCAS constructs, and Weijun Feng and Patricia Rusu for critical reading of the manuscript. This work was supported by the Helmholtz Association (VH-NG-702), the Deutsche Forschungsgemeinschaft (LI 2140/1-1), the Deutsche Krebshilfe (110226), the Helmholtz Alliance Preclinical Comprehensive Cancer Center (PCCC), and the DKFZ Intramural Grant Program. This work was also supported in part by a grant from the DKFZ-Bayer Healthcare Alliance.

Received: December 15, 2012
Revised: December 3, 2013
Accepted: April 10, 2014
Published: May 15, 2014

REFERENCES

Barrett, L.E., Granot, Z., Coker, C., Iavarone, A., Hambardzumyan, D., Holland, E.C., Nam, H.S., and Benezra, R. (2012). Self-renewal does not predict tumor growth potential in mouse models of high-grade glioma. Cancer Cell *21*, 11–24.

Belz, T., Liu, H.K., Bock, D., Takacs, A., Vogt, M., Wintermantel, T., Brandwein, C., Gass, P., Greiner, E., and Schütz, G. (2007). Inactivation of the gene for the nuclear receptor tailless in the brain preserving its function in the eye. Eur. J. Neurosci. *26*, 2222–2227.

Bickenbach, J.R. (1981). Identification and behavior of label-retaining cells in oral mucosa and skin. J. Dent. Res. *60 Spec No C* (Spec No), 1611–1620.

Brill, M.S., Snapyan, M., Wohlfrom, H., Ninkovic, J., Jawerka, M., Mastick, G.S., Ashery-Padan, R., Saghatelyan, A., Berninger, B., and Götz, M. (2008). A dlx2- and pax6-dependent transcriptional code for periglomerular neuron specification in the adult olfactory bulb. J. Neurosci. *28*, 6439–6452.

Chen, J., Li, Y., Yu, T.S., McKay, R.M., Burns, D.K., Kernie, S.G., and Parada, L.F. (2012). A restricted cell population propagates glioblastoma growth after chemotherapy. Nature *488*, 522–526.

Clevers, H. (2011). The cancer stem cell: premises, promises and challenges. Nat. Med. *17*, 313–319.

Corsini, N.S., Sancho-Martinez, I., Laudenklos, S., Glagow, D., Kumar, S., Letellier, E., Koch, P., Teodorczyk, M., Kleber, S., Klussmann, S., et al. (2009). The death receptor CD95 activates adult neural stem cells for working memory formation and brain repair. Cell Stem Cell *5*, 178–190.

Driessens, G., Beck, B., Caauwe, A., Simons, B.D., and Blanpain, C. (2012). Defining the mode of tumour growth by clonal analysis. Nature *488*, 527–530.

Feng, W., Khan, M.A., Bellvis, P., Zhu, Z., Bernhardt, O., Herold-Mende, C., and Liu, H.K. (2013). The chromatin remodeler CHD7 regulates adult neurogenesis via activation of SoxC transcription factors. Cell Stem Cell *13*, 62–72.

Furnari, F.B., Fenton, T., Bachoo, R.M., Mukasa, A., Stommel, J.M., Stegh, A., Hahn, W.C., Ligon, K.L., Louis, D.N., Brennan, C., et al. (2007). Malignant astrocytic glioma: genetics, biology, and paths to treatment. Genes Dev. *21*, 2683–2710.

Gil, J., and Peters, G. (2006). Regulation of the INK4b-ARF-INK4a tumour suppressor locus: all for one or one for all. Nat. Rev. Mol. Cell Biol. *7*, 667–677.

Gong, S., Zheng, C., Doughty, M.L., Losos, K., Didkovsky, N., Schambra, U.B., Nowak, N.J., Joyner, A., Leblanc, G., Hatten, M.E., and Heintz, N. (2003). A gene expression atlas of the central nervous system based on bacterial artificial chromosomes. Nature *425*, 917–925.

He, S., Nakada, D., and Morrison, S.J. (2009). Mechanisms of stem cell self-renewal. Annu. Rev. Cell Dev. Biol. *25*, 377–406.

Holland, E.C. (2001). Gliomagenesis: genetic alterations and mouse models. Nat. Rev. Genet. *2*, 120–129.

Holland, E.C., Hively, W.P., DePinho, R.A., and Varmus, H.E. (1998). A constitutively active epidermal growth factor receptor cooperates with disruption of G1 cell-cycle arrest pathways to induce glioma-like lesions in mice. Genes Dev. *12*, 3675–3685.

Kay, M.M. (1975). Mechanism of removal of senescent cells by human macrophages in situ. Proc. Natl. Acad. Sci. USA *72*, 3521–3525.

Kretzschmar, K., and Watt, F.M. (2012). Lineage tracing. Cell *148*, 33–45.

Li, L., and Clevers, H. (2010). Coexistence of quiescent and active adult stem cells in mammals. Science *327*, 542–545.

Liu, H.K., Belz, T., Bock, D., Takacs, A., Wu, H., Lichter, P., Chai, M., and Schütz, G. (2008). The nuclear receptor tailless is required for neurogenesis in the adult subventricular zone. Genes Dev. *22*, 2473–2478.

Liu, H.K., Wang, Y., Belz, T., Bock, D., Takacs, A., Radlwimmer, B., Barbus, S., Reifenberger, G., Lichter, P., and Schütz, G. (2010). The nuclear receptor tailless induces long-term neural stem cell expansion and brain tumor initiation. Genes Dev. *24*, 683–695.

Magee, J.A., Piskounova, E., and Morrison, S.J. (2012). Cancer stem cells: impact, heterogeneity, and uncertainty. Cancer Cell *21*, 283–296.

Monaghan, A.P., Grau, E., Bock, D., and Schütz, G. (1995). The mouse homolog of the orphan nuclear receptor tailless is expressed in the developing forebrain. Development *121*, 839–853.

Nam, H.S., and Benezra, R. (2009). High levels of Id1 expression define B1 type adult neural stem cells. Cell Stem Cell *5*, 515–526.

Reya, T., Morrison, S.J., Clarke, M.F., and Weissman, I.L. (2001). Stem cells, cancer, and cancer stem cells. Nature *414*, 105–111.

Rowland, B.D., and Peeper, D.S. (2006). KLF4, p21 and context-dependent opposing forces in cancer. Nat. Rev. Cancer *6*, 11–23.

Schepers, A.G., Snippert, H.J., Stange, D.E., van den Born, M., van Es, J.H., van de Wetering, M., and Clevers, H. (2012). Lineage tracing reveals Lgr5+ stem cell activity in mouse intestinal adenomas. Science *337*, 730–735.

Shah, N.M., Groves, A.K., and Anderson, D.J. (1996). Alternative neural crest cell fates are instructively promoted by TGFbeta superfamily members. Cell *85*, 331–343.

Sharpless, N.E., and DePinho, R.A. (2007). How stem cells age and why this makes us grow old. Nat. Rev. *8*, 703–713.

Shi, Y., Chichung Lie, D., Taupin, P., Nakashima, K., Ray, J., Yu, R.T., Gage, F.H., and Evans, R.M. (2004). Expression and function of orphan nuclear receptor TLX in adult neural stem cells. Nature *427*, 78–83.

Singec, I., Knoth, R., Meyer, R.P., Maciaczyk, J., Volk, B., Nikkhah, G., Frotscher, M., and Snyder, E.Y. (2006). Defining the actual sensitivity and specificity of the neurosphere assay in stem cell biology. Nat. Methods *3*, 801–806.

Singh, S.K., Clarke, I.D., Terasaki, M., Bonn, V.E., Hawkins, C., Squire, J., and Dirks, P.B. (2003). Identification of a cancer stem cell in human brain tumors. Cancer Res. *63*, 5821–5828.

Singh, S.K., Hawkins, C., Clarke, I.D., Squire, J.A., Bayani, J., Hide, T., Henkelman, R.M., Cusimano, M.D., and Dirks, P.B. (2004). Identification of human brain tumour initiating cells. Nature *432*, 396–401.

Snippert, H.J., van der Flier, L.G., Sato, T., van Es, J.H., van den Born, M., Kroon-Veenboer, C., Barker, N., Klein, A.M., van Rheenen, J., Simons, B.D., and Clevers, H. (2010). Intestinal crypt homeostasis results from neutral competition between symmetrically dividing Lgr5 stem cells. Cell *143*, 134–144.

Sun, G., Yu, R.T., Evans, R.M., and Shi, Y. (2007). Orphan nuclear receptor TLX recruits histone deacetylases to repress transcription and regulate neural stem cell proliferation. Proc. Natl. Acad. Sci. USA *104*, 15282–15287.

Vescovi, A.L., Galli, R., and Reynolds, B.A. (2006). Brain tumour stem cells. Nat. Rev. Cancer *6*, 425–436.

Zhang, C.L., Zou, Y., Yu, R.T., Gage, F.H., and Evans, R.M. (2006). Nuclear receptor TLX prevents retinal dystrophy and recruits the corepressor atrophin1. Genes Dev. *20*, 1308–1320.

Zhang, C.L., Zou, Y., He, W., Gage, F.H., and Evans, R.M. (2008). A role for adult TLX-positive neural stem cells in learning and behaviour. Nature *451*, 1004–1007.

Zou, Y., Niu, W., Qin, S., Downes, M., Burns, D.K., and Zhang, C.L. (2012). The nuclear receptor TLX is required for gliomagenesis within the adult neurogenic niche. Mol. Cell. Biol. *32*, 4811–4820.